IPPJ-AM-31

ATOMIC PROCESSES IN HOT DENSE PLASMAS

T. KAGAWA, T. KATO, T. WATANABE
AND S. KARASHIMA

INSTITUTE OF PLASMA PHYSICS
NAGOYA UNIVERSITY

NAGOYA, JAPAN

IPPJ-AM-31

ATOMIC PROCESSES IN HOT DENSE PLASMAS

Takashi KAGAWA[1)], Takako KATO, Tsutomu WATANABE[2)]
and Shosuke KARASHIMA[3)]

Institute of Plasma Physics, Nagoya University
Chikusa-ku, Nagoya 464, Japan

August 1983

Permanent address:

1) Department of Physics, Nara Women's University
2) The Institute of Physical and Chemical Research
3) Faculty of Engineering, Science University of Tokyo

Abstract

The central-field models and the theoretical analyses for some atomic processes in hot, dense plasmas are reviewed. The qualitative trends of the density- and temperature-dependent properties of plasma particles, which could be used for diagnostics of the plasma, are described.

§1. INTRODUCTION

Hot, dense plasmas have vigorously been studied in various fields in physics such as plasma physics, astrophysics, atomic physics and solid state physics, in particular in connection with the inertia confinement fusion (ICF) study.

In the ICF research, description of the plasma under extreme conditions such as high temperature ($T \gtrsim 10^6$ K) and high density ($N_e \gtrsim 10^{24}$ /cm^3) in terms of the microscopic atomic processes is required when modelling the plasma. Since the ICF plasma is usually produced in a very short-time scale ($\approx 10^{-9}$ sec), it is neither homogeneous nor steady. This means that the motion of nonthermal electrons and ions accompanying mutual collision or indirect interaction through the emission and absorption of photons determines the density and temperature in each position and time. This situation is very different from low density plasmas observed in solar corona or the Tokomak, where the effect of the surrounding plasma on a test atom can be considered to be a small perturbation. These low density plasmas, where collision processes are dominant, have been studied by use of the perturbation theory for the atomic processes in the plasma.

Modification of the models based on the thermal equilibrium such as corona equilibrium or the local thermal eqilibrium (LTE) may be required in the study of an unsteady plasma such as the ICF one. Moreover, one has to introduce the molecular or solid-state effects into the model in describing the atomic properties of ions in dense plasmas, since the average internuclear distance in these plasmas becomes much smaller than that in the normal solid state: The radii of most atomic orbitals are larger than the internuclear distance.

A large number of papers on hot, dense plasmas so far been published concern with a variety of subjects such as radiation or particle transport processes, plasma spectroscopy, equation of states, atomic processes, etc.. One component plasma has extensively been studied as an ideal system (Ichimaru 1977).

Even if one confines the subjects to problems in diagnosing hot, dense plasmas through the analysis of the line broadening and line shift in X-ray spectra observed, there are two main themes related to atomic physics. One is the structure of ions in a plasma as a source of light and the other is the atomic processes related to energy transport and opacity. Various models with the assumption of the thermal equilibrium for the plasmas have been proposed. Most of them are the central-field atomic model which yields the single-electron energies of ions in a plasma.

This note presents a brief survey on the atomic models and the qualitative trends of the density- and temperature-dependent properties of ions in a hot, dense plasma. Recently some review papers on atomic physics in hot, dense plasma have been published (More, 1981, Weisheit 1981, Gupta and Rajagopal, 1982; papers in JQSRT 27, 1982). Details of the studies on dense plasmas including the subject on energy transport and opacity can be found in these articles.

§2. CENTRAL-FIELD MODELS FOR ATOMS IMMERSED IN A PLASMA

A test charge immersed in a plasma receives various types of the perturbations from surrounding plasma particles. One of significant perturbations is the screening of the nuclear charge by free electrons as a result of the plasma polarization effect, i.e. departure from the uniform distribution of electrons and ions near the test charge. Another is the fluctuation of the microfield around the test charge due to the instantaneous motion of ions and electrons and their collective motion called as the plasma oscillation. In addition to these effects, the perturbation due to electron impact is also an important factor to characterize the level population or life time of excited states of the ion especially for low-density plasmas.

As the density of a plasma increases, the screening of the nuclear charge by free electrons becomes significant. On the other hand, this effect of the screening decreases when the temperature becomes high, since the ion can move freely over the potential barrier due to the surrounding plasma media. In order to specify such plasma condition instead of two parameters of the density and temperature, one often uses a dimensionless plasma parameter Γ which is the ratio of the average Coulomb energy for ions to the temperature of the plasma, defined as

$$\Gamma = \frac{Z_i^* e^2}{R_i kT} \quad , \tag{1}$$

where Z_i^* and R_i are the avearge charge and ion-sphere radius of ions, respectively. The ion-sphere radius is given by

$$R_i = \left(\frac{3Z_i^*}{4\pi N_e}\right)^{\frac{1}{3}} \quad , \tag{2}$$

where N_e is the electron density.

The structure of a test atom immersed in a plasma has extensively been investigated by using the central-field models with appropriate electrostatic potentials for the atom. The electrostatic potential V is obtained as a solution of the Poisson equation written as

$$\nabla^2 V = -4\pi e\rho \tag{3}$$

if the average charge distribution both the positive and negative charges around the atom with an appropriate model is given. Since the average charge distribution ρ in Eq. (3) heavily depends on the plasma condition, there certainly exists a critical condition at which a particular model breaks down. In the following, various central-field models used in dignosing a plasma are described briefly.

2-a) Debye-Hückel Model

This model starts with the non-uniform statistical distribution of the charged particles around a test charge Ze. Using Boltzmann's law, the number of a-th particle having the charge $Z_a e$ as a function of r is written as

$$N_a(r) = N_{a0} \exp\left[-\frac{Z_a e}{kT_a} V(r)\right] \tag{4}$$

where N_{a0} is the uniform value and V(r) is the electrostatic potential. The DH average charge distribution $\rho_{DH}(r)$ can be obtained as

$$\rho_{DH}(r) = e\sum_a Z_a N_a(r) = e\sum_a Z_a N_{a0} \exp\left[-\frac{Z_a e}{kT_a} V(r)\right] \quad . \tag{5}$$

The condition that a plasma be neutral leads to the following relation,

$$\sum_a Z_a N_a = 0 \quad . \tag{6}$$

The exponetial part in Eq. (5) can be expanded to the first-order of V under the condition that $kT \gg |V|$, i.e. $\Gamma \ll 1$. By inserting this linearized $\rho_{DH}(r)$ with respect to V into Eq. (3), the DH potential $V_{DH}(r)$ is obtained in the familiar form,

$$V_{DH}(r) = \frac{Ze^2}{r} e^{-\frac{r}{D}} \quad , \tag{7}$$

where D, the Debye length, is given by

$$D = \frac{1}{[4\pi e^2 (\sum_a Z_a^2 N_{a0})/kT]^{1/2}} \tag{8}$$

The DH potential could be a good approximation for low density and high temperature plasmas because of the linearlized $\rho_{DH}(r)$.

2-b) Ion-Sphere (IS) Model

In a strongly compressed plasma, the density of the free electrons around the ion is very high. The ion-sphere (IS) model is constructed from the assumption that electrons are uniformly distributed in the ion sphere, so that $\rho_{IS}(r)$ is written as

$$\rho_{IS}(r) = \begin{cases} Z/(\frac{4\pi}{3} R_i^3) , & \text{when} \quad r \leqq R_i . \\ 0 , & \text{when} \quad r > R_i \end{cases} \tag{9}$$

where R_i is the ion sphere radius. The IS potential is obtained by use of the Poisson equation in the following form,

$$V_{IS}(r) = \begin{cases} \frac{Ze}{r} - \frac{Ze}{2R_i} (3 - \frac{r^2}{R_i^2}), & \text{when} \quad r \leqq R_i , \\ 0 , & \text{when} \quad r > R_i \end{cases} \tag{10}$$

It is noted that R_i depends only on the density of the plasma. However, as nuclei are assumed to be fixed in this model, it can be expected that this model yields good results for low temperature and high density plasmas.

2-c) Thomas-Fermi (TF) Model

This model is one of the ion-sphere models which are suitable for dense plasmas. The TF theory at zero temperature has well been known to be useful in the study of highly compressed matter, since the atomic electrons can be confined within an atomic sphere by introducing the cut off condition for the electron distribution, where the charge at the boundary remains non-zero. The zero-temperature TF theory has been extended to the finite temperature TF theory by some authors (Feynman et. al. 1949 and Cowan et. al. 1957). If one replaces the atomic electrons in a sphere by the finite-temperature semi-classical gas, the TF distribution $\rho_{TF}(r)$ is written as

$$\rho_{TF}(r) = \frac{8\pi}{h^3} \int_0^\infty \frac{P^2 dP}{\exp[(\frac{P^2}{2m} - eV(r) - \mu)/kT] + 1} , \tag{11}$$

where the chemical potential μ is determined by the requirement that the cell be neutral:

$$\int \rho_{TF}(r) d^3r = Z . \tag{12}$$

By solving Eq. (11) and Eq. (3) self-consistently, the $V_{TF}(r)$ is obtained numerically. The TF theory has widely been applied to the dense plasmas with various modifications.

2-d) Average Atom (AA) Model

The average atom model (Chandrasecker 1939) is essetially based upon the assumption that atomic electrons are distributed in the single-electron levels according to the Fermi statistics. This assumption leads to the non-integer occupation number for the $n\ell$ state given by

$$N_{n\ell} = \frac{2(2\ell + 1)}{\exp[(\varepsilon_{n\ell} - \mu)/kT] + 1} , \tag{13}$$

where $\varepsilon_{n\ell}$ is the orbital energy. The single-electron levels for an atom can be obtained as solutions of the Schrödinger equation with an appropriate screened potential. The average atom model has been used for plasma modelling because of its simple and unified treatment of the structure for various ionization stages of an ion immersed in a plasma.

However, this model cannot be used to identify the lines from atoms in different ionization stages or to calculate the ratio of intensities for lines because this model leads to a fictious atom which consists of the average of all the possible ionization stages of the real atom.

2-d-1) Self-Consistent-Field-Average-Atom (SCFAA) Model

Rozsnyai (1972) has proposed a self-consistent-field-average-atom (SCFAA) model, where all electrons are assumed to be confined within a sphere having the radius R_i. The relativistic Hartree-Fock-Slater (RHFS) method is used to determine the single-electron levels for the bound electrons. The density of the bound electrons ρ_b is calculated with the RHFS orbitals and the Fermi distribution function. On the other hand, density of free electrons ρ_f is determined by use of the relativistic expression of the finite temperature TF theory. The total potential including the exchange and the correlation potentials is calculated using ρ_b and ρ_f. This total potential written as

$$V(r) = \frac{Ze}{r} + V_b(r) + V_f(r) + V_{ex}(r) + V_{corr}(r) \tag{14}$$

is used in the RHFS equation. The calculation terminates when the self-consistent potential is obtained. This model has been used to calculate various physical quantities of ions in a hot, dense plasma such as the line shift and the photoabsorption cross section by Rozsnyai.

2-d-2) Screened Hydrogenic Ionization (SHI) Model

Application of the semi-clasical WKB theory to hydrogenic systems yields analytic expressions for the energy and expectation values for the coordinate or momentum operators. These expressions except for the energy are different from those obtained with the quantum mechanics. The screened hydrogenic ionization (SHI) model (More 1981) is an extension of the WKB results for hydrogenic systems to many-electron atoms, where the effective charges are introduced into the WKB expression for the energy so that it becomes a good approximation for each orbital energy in many-electron atoms. In this model, the sub-shell splitting of orbital energies between $n\ell$ and $n\ell'$ is neglected. The SHI orbital energy with a principal quantum number n for an atom has the form

$$E_n = E_n^0 - \frac{Q_n^2 e^2}{2a_0 n^2} \quad , \tag{15}$$

where E_n^0 is the energy-shift with outer screening, Q_n is the effective charge due to the inner screening and a_0 is the Bohr radius. In the WKB approximation, a shell is expressed by a classical orbit with the radius r_n as

$$r_n = \frac{a_0 n^2}{Q_n} \quad . \tag{16}$$

Q_n depends on the electron population $\{P_m\}$ of the shells inside r_n, whereas E_n^0 depends on $\{P_m\}$ of the shells outside r_n. This dependence of Q_n and E_n^0 are represented with a linear approximation with respect to P_m as

$$Q_n = Z - \sum_{m<n} \sigma(n,m)\, P_m - \frac{1}{2}\sigma(n,n)\, P_n \tag{17}$$

and

$$E_n^0 = \frac{1}{2}\, \frac{e^2}{r_n}\, \sigma(n,n)\, P_n + \sum_{m>n} \frac{e^2}{r_m}\, P_m\, \sigma(m,n)\,, \tag{18}$$

where $\sigma(n,m)$ is the screening coefficient which describes the screening of the n-th shell by the m-th shell electrons. A set of screening coefficients $\{\sigma(m,n)\}$ can be calculated using the first-order perturbation theory for hydrogenic wavefunctions.

The SHI model essentially deals with a set of electron populations of various shells $\{P_m\}$ combined with screening coefficients $\{\sigma(m,n)\}$. If the thermal equilibrium is assumed for a plasma, the average population (occupation) number $\overline{P_n}$ may be written as

$$\overline{P}_n = \frac{2n^2}{\exp[(E_n - \mu)/kT] + 1} \quad . \tag{19}$$

This model has also been applied to diagnostics of the non-LTE plasmas such as the ICF one because the much reduction of the calculation for such a complex system is possible with this model.

2-e) Intermediate Models

The limitation of the DH model is that it can be applied only to low-density and high-temperature plasmas, whereas the IS model is a good approximation for high-density and low-temperature ones. There are some models which cover the intermediate plasma conditions, where both the DH and the IS models are not valid. Here, the Thomas-Fermi-ion-core (TFIC) model (Stwert and Pyatt 1966) and the effective screening model (Singwi 1977; Gupta and Rajagopal 1979) are described.

2-e-1) TFIC Model

In the ion-sphere (IS) model, each ion has the ion sphere which contains enough free electrons to maintain charge neutrality in the sphere. However, the effect of the position correlation between ions moving in various positions is not contained in this model. The TFIC model consists of the TF model for free electrons, the average atom (AA) model for bound electrons and the Maxwell-Boltzmann distribution for neighboring ions. The total charge distribution $\rho(r)$ is expressed as a sum of the charge distributions for bound electrons $\rho_b(r)$, free electrons $\rho_f(r)$ and neighboring ions $\rho_i(r)$ in the following,

$$\rho(r) = \rho_b(r) + \rho_f(r) + \rho_i(r) \quad ; \tag{20}$$

where

$$\rho_b(r) = \frac{1}{4\pi}\sum_{n,\ell} \frac{2(2\ell+1)}{\exp[(\mathcal{E}_{n\ell}-\mu)/kT_e]+1}|R_{n\ell}(r)|^2 \quad , \tag{21}$$

$$\rho_f(r) = \frac{8\pi}{h^3}\int_0^\infty \frac{P^2\,dP}{\exp[(\frac{P^2}{2m} - eV(r) - \mu)/kT_e + 1} \tag{22}$$

and

$$\rho_i(r) = \rho_{i0}\exp\left[-\frac{Ze}{kT_i}V(r)\right] \quad . \tag{23}$$

The radial part of the wave function $R_{n\ell}(r)$ is obtained as a solution of the Schrodinger equation using the potential $V(r)$. The Poisson equation (3) and Eqs. (20)-(23) combined with the Schrödinger equation are solved iteratively until the self-consistent solution for $\rho(r)$ and $V(r)$ is obtained. This model has been used to explain the lowering of the ionization potential in the intermediate region of the plasma conditions (Stwert et. al. 1966).

2-e-2) Effective Screening Model

The effective screening model deals with the effective potential which is obtained through the density functional approach for the formulation of the free-energy framework. The effective screening potential (Gupta et. al. 1979) is expressed as

$$V_{eff}(r, n_e, T_e) = \frac{2e}{\pi}\int_0^\infty dq \left(\frac{\sin qr}{qr}\right) \frac{1}{1 - (4\pi e^2/q^2)\chi(q, n_e, T_e)} , \tag{24}$$

where $\chi(q,n,T)$, the RPA Lindhard function, is given by

$$\chi(q, n, T) = -2\int \frac{d^3P}{(2\pi\hbar)^3} \frac{f(p+q) - f(p)}{\frac{p^2}{2m} - \frac{(p+q)^2}{2m}} \tag{25}$$

and

$$f(p) = \frac{1}{\exp[(\frac{p^2}{2m} - \mu)/kT] + 1} \tag{26}$$

For $q \to 0$ limit in Eq. (24), $V_{eff}(r)$ reduces to the screened Coulomb potential with the effective screening parameter $\xi(n_e, T_e)$ in the followung form,

$$V_{eff}(r, n_e, T_e) \xrightarrow[q \to 0]{} V_\xi(r) = \frac{Ze^2}{r} e^{-\xi(n_e, T_e)\cdot r} \quad . \tag{27}$$

The parameter $\xi(n_e, T_e)$ also reduces to a constant corresponding to the DH and the TF values for high temperature and low temperature limits, respectively:

$$\xi(n_e, T_e) \xrightarrow[T_e \to \infty]{} \xi_{DH} \tag{28}$$

and

$$\xi(n_e, T_e) \xrightarrow[T_e \to 0]{} \xi_{TF} \quad . \tag{29}$$

§ 3. STRUCTURE OF IONS AND ATOMIC PROCESSES

In this section, the density and temperature effects on the structure of ions and some atomic processes in hot, dense plasmas are described.

3-a) Energy Levels

As the nuclear charge is fairly screened in the DH potential, the values of the most screened potentials based on the corresponding central-field model described in § 2 as a function of r always lie between those of the DH and the pure Coulomb potentials. The single-electron energies for ions are obtained as solutions of the Schrödinger equation with these potentials.

The shield of the nuclear charge leads to a short range potential which allows only a finite number of bound states. This means that highly excited bound states (Rydberg states) for a pure Coulombic potential dissolve into the continuum sea of states in the system. This fact is known as 'continuum lowering' or 'pressure ionization' as a result of the screening of the nuclear charge by free plasma electrons. In addition to the continuum lowering of energy levels, separation of the energy between neighboring states decreases as the screening of the nuclear charge increases. A screened Coulomb potential yields the sub-shell splitting of the energy levels belonging to the $n\ell$ states for which azimuthal quantum numbers are different. The same type of the splitting of energy levels is always observed in the Hartree-Fock (HF) orbital energies of an isolated atom since the HF potential is a non-Coulombic potential.

Although the DH model is a good approximation for low density and high temperature plasmas, it has been examined over a wide range of the plasma conditions by some authors (Rogers et. al. 1971, Roussel et. al. 1974). The dependence of the DH energy levels of lower-lying and higher-lying states on the screening lengths (Rogers et. al, 1971) is shown in Fig. 1 and 2, respectively. Characteristic behaviors of the bound levels such as the continuum lowering and the decrease of the spacing of energy levels mentioned above are seen from these figures. It is also seen that no bound state, as is expected, exists in the high-density limit.

3-b) Oscillator Strength and Photoabsorption Cross Section

The absorption oscillator strength $f(b \leftarrow a)$ and the spontaneous emmision rate $A(b \rightarrow a)$ are related to the opacity and line strengths of the observed spectra. The oscillator strength $f(b \leftarrow a)$ is connected with the spontaneous emission rate $A(b \rightarrow a)$ through the relation,

$$f(b \leftarrow a) = \frac{2m\omega_{ba}}{3\hbar} |\langle b|\vec{r}|a\rangle|^2 = \frac{mc^3}{2e^2\omega_{ba}} A(b \rightarrow a) \ , \tag{30}$$

where m is the electron mass, c is the velocity of light, ω_{ba} is the transition frequency and $\langle b|\vec{r}|a\rangle$ is the transition matrix element in the dipole approximation.

The f-value or the A-value for bound-bound transitions as a function of the density and temperature has been calculated with the DH potential for hydrogenic systems (Roussel et. al. 1974, Weisheit et. al. 1974, Shore 1975 and Höhne et. al. 1982). They showed that the f-value or the A-value for a transition decreases rapidly when the Debye screening length becomes as small as a few times the critical screening length of the upper level. This is shown in Fig. 3. Weisheit and Shore (1974) have calculated the oscillator strengths and photoabsorption cross sections for the $1s \rightarrow np$ transition for all the bound and continuum states using the DH model. The calculated results of them show that the decrease and sudden drop of the f-value at the threshhold energy.

Höhne et. al. (1982) re-examined the behavior of the oscillator strength for the bound-bound and bound-free transitions and claimed the results of Weisheit and Shore, namely, the drastic reduction of the oscillator strength at threshhold, where the smooth connection of the f-value between the bound-bound and bound-free transitions around the threshhold was not observed. The conclusion of Höhne et. al. is that the averaged oscillator strength given by

$$\sigma_{n\ell}(\omega) = \sum_{\ell'=\ell\pm1} f_{n\ell,\, q'\ell'} \left(dE_{q'\ell'}/dq'\right)^{-1} \Big|_{\hbar\omega = E_{q'\ell'} - E_{n\ell}} \tag{31}$$

should be used for a non-Coulombic potential such as the DH one, since the application of the Coulomb result for the differential oscillator strength df/dE to non-Coulombic systems leads to an incorrect resutlt. The calculated results of the averaged oscillator strengths $\sigma_{n\ell}(\omega)$ for the DH potential by Höhen et. al. are shown in Fig. 4 together with those for the pure Coulomb potential. It is seen from Fig. 4 that the curve of $\sigma_{n\ell}(\omega)$ for the DH and the pure Coulomb potentials are very close to each other.

Characteristic behavior of the photoabsorption cross section for a screened potential is the $k^{2\ell+1}$ behavior near the threshhold energy (Wigner 1948). Shore (1975), however, showed that since near-resonant wavefunctions for energies with a narrow interval between the DH and the pure Coulomb threshholds have the enhanced amplitude within the potential well interior, the photoabsorption cross section increases in this region of the photon energy. The same result has also been obtained by Höhne et. al. (1982).

3-c) Shift of Spectral Lines

The shift of spectral lines has been calculated with various atomic models for an emissive ion in a plasma. As has been mentioned before, the energy difference between the states decreases as the screening of the nuclear charge by free electrons increases. This means that the lines are shifted toward the lower frequency side, that is, the red shift. On the other hand, the the plasma polarization shift (PSS) theory (Griem 1974) which deals with the effective charge of the ion using the perturbation theory gives the blue shift for the resonance line of the hydrogenic helium ion.

Skupsky (1980) has calculated the magnitude of the line shift with the modified Thomas-Fermi-ion-core (TFIC) model for the $2p \to 1s$ transition of a hydrogenic impurity neon in deutrium and tritium plasma, where the charge distribution of the bound electron is obtained with the statistical average of the $|\psi_{1s}|^2$ and $|\psi_{2p}|^2$. The calculated shifts of the Lyman-α line for hydrogenic neon in the plasma are compared with those using the DH, the IS and the effective screening models in Fig. 5. In the low density limit, Skupsky's result shows the characteristic oscillation and the blue shift. However, in the high density limit, the line shift with his model becomes the red shift which is the same trend of the line shift as other models such as the DH one. This behavior of the line shift, namely, the blue shift in the low density limit and the red shift in the high density limit has been confirmed by the SCFAA calculation (Rozsnyai 1975). In Fig. 5, the calculated results with different models (Cauble 1982, Gupta et. al. 1981) are also compared. Cauble's result is based on the plasma polarization shift theory, while Gupta et. al. used the effective screening model. These calculations of the line shift for hydrogenic neon in a hydrogen plasma give the red shift with the intermediate values between that of Skupsky and the DH value for all densities of the plasma considered.

Concerning the profile of spectral lines, there have been proposed some methods other than the plasma polarization shift theory (Griem 1974) to calculate both the shift and width of lines at the same time. The problems of the broadening of the spectral lines are closely related to opacity in hot, dense plasmas. Using the perturbation expansion of the partition function for the multicomponent plasmas, Nakayama et. al. (1964) has derived a pseudo-Schrödinger equation containing the complex potential. Yamamoto et. al. (1980) have studied the complex level shift which incldes both the shift and width, with the quantum scattering theory based on the impact approximation. However, it seems that problems lie in the application of such method based on the perturbation theory to dense plasmas.

3-d) Free-Free Transition

Free-free transitions are important processes in problems for the transport and loss of the radiation in plasmas. Especially, the free-free photoabsorption plays an important role in heating plasmas by laser.

The cross section σ for the free-free transition is often expressed by the Gaunt factor G as

$$G = \sigma/\sigma_{cl} \ , \tag{32}$$

where σ_{cl} is the Kramers classical cross section,

$$\sigma_{cl} = \frac{16\pi}{3\sqrt{3}} \alpha^3 \frac{\hbar^2}{2m} \frac{Z^2}{W_0 h\nu} \ . \tag{33}$$

Here, α is the fine structure constant, W_0 is the energy of the incident electron and ν is the frequency of the photon emitted. The general expression for G in the non-relativistic Born approximation has been given by Grant (1958).

The Gaunt factor can be obtained in an analytic form if an analytic form such as the Yukawa-type function is assumed for the electron-ion potential in the Born approximation. Suppose the potential V(r) is constructed as a superposition of the two Yukawa-type potentials, given by

$$V(r) = e \left[\frac{Z - N_b}{r} e^{-\alpha r} + \frac{N_b}{r} e^{-\beta r} \right] \ , \tag{34}$$

where Z is the nuclear charge, N_b is the average number of bound electrons and α and β are screening parameters, the Gaunt factor G has the following analytic form,

$$G = g(q_{max}) - g(q_{min}) \; , \tag{35}$$

where

$$g(q) = \frac{\sqrt{3}}{\pi}\left[-\frac{q^2}{2(q^2+\alpha^2)} + \frac{1}{2}\ln(q^2+\alpha^2)\right.$$
$$+ \frac{N_b^2}{(Z-N_b)^2}\left\{-\frac{q^2}{2(q^2+\beta^2)} + \frac{1}{2}\ln(q^2+\beta^2)\right\}$$
$$+ \frac{1}{2}\frac{N_b}{(Z-N_b)}\left\{\ln(q^4+q^2\alpha^2+q^2\beta^2+\alpha^2\beta^2)\right.$$
$$\left.\left. + \frac{\beta^2+\alpha^2}{\beta^2-\alpha^2}\ln\frac{q^2+\beta^2}{q^2+\alpha^2}\right\}\right]. \tag{36}$$

q_{max} and q_{min} mean the maximum and minimum values of the momentum transfer q, respectively.

Rozsnyai (1979) has derived Eq. (36) and calculated the Gaunt factor averaged over the energy distribution of the free electrons in cecium plasmas at T_e= 100 eV and 1 KeV, using the potential in a form of Eq. (34) where the parameters α and β were determined so that the values of V(r) becomes the same as those of the SCFAA potential at two chosen points of r. His results show that the Gaunt factor increases in the high energy photon region and decreases in the soft photon region as the density becomes high. When the density increases, the relative drop of the Gaunt factor toward the low-frequency side of the photon energy is observed, since available upper states decrease.

Recently Lamoureux et. al. (1982) have investigated the free-free emission in a cesium plasma of the normal density at kT=1 keV. They have calculated the Gaunt factor not only in the Born approximation but also with the relativistic partial wave expansion method using both the Thomas-Fermi potential V_{TF} and the SCFAA one V_{SCFAA} obtained by Rozsnyai (1979) for this system. The calculated results at W_0=1 keV are shown in Fig. 6. The values of G^B were obtained with the Elwert factor in the Coulomb Born approximation. It is noted that the Born-Elwert approximation for G is valid in a relatively wide range of the incident electron energies comparing with the Born approximation. $G^B{}_{SCFAA}$ denotes the results obtained with the expression for the Gaunt factor in Eq. (35). G_{TF} and G_{SCFAA} indicate the results based on the relativistic partial wave expansion method for V_{TF} and V_{SCFAA} , respectively.

It is seen from Fig. 6 that values of G^B_{SCFAA} are smaller than those of G^B. This indicates that the screening of the nuclear charge by electrons reduces the Gaunt factor. The calculated results of G^B_{SCFAA} in the Born approximation, however, are large compared with those of G_{SCFAA} using the numerical partial wave method, although the same SCFAA potential is used. This fact shows the importance of the mothod of calculation rather than the potential in the calculation of the Gaunt factor.

3-e) Collision Processes Between an Electron and an Ion

When an ion with the nuclear charge Ze and N electrons is immersed in a hot, dense plasma, the electronic excitation process of the ion by the collision of an incomming electron,

$$e + A^{q+} \rightarrow e + (A^{q+})^* \qquad (37)$$

and

$$q = Z - N \qquad (38)$$

is significantly affected by the presence of the positive and negative charges near the ion. In vacuum, the excitation of an ion by electron impact is treated as the collision process strongly influenced by the long range Coulomb potential between the electron and the ion. In a hydrogen plasma, we should take into account the effect of the electrostatic potential due to electrons and protons. Usually some of these electrons move slower and others faster, as compared with speed of the impact electron. Both electrons and protons form the spherically asymmetric potentials for the projectile electrons.

At present, no trial has been made for the estimation of the electronic excitation cross section which includes such time dependent, spherically asymmetric potential effects. Only the approaches using the averaged spherically symmetric potential have been made for the excitation processes of one-electron ion with the charge Ze (Hatton, Lane and Weisheit, 1981) and the same processes for Z=10, i.e.,

$$e + Ne^{9+} \rightarrow e + (Ne^{9+})^* \qquad (39)$$

In the paper of Hatton et. al. (1981), the electron-ion interaction was assumed to be the following form of the exponetially screened Coulomb potential:

$$V(\vec{r_1},\vec{r_2}) = \left(\frac{Ze}{r_1} - \frac{e}{|\vec{r_1} - \vec{r_2}|}\right) \exp\left(-\frac{r_1}{D}\right), \tag{40}$$

where D is the Debye-Hückel screening length, given in Eq. (8), $\vec{r}_1$ and $\vec{r}_2$ are the position vectors of the projectile electron and the bound electron, respectively. The cross sections for the 1s → 2s and the 1s → 2p excitations have been obtained. In the relation between the collision strength Ω and the incident kinetic energy E, the scaling relation of $Z^2\Omega$ and E/Z^2 gives general schemes. The curves of the collision strength for the 1s → 2s and the 1s → 2p excitation processes are shown in Fig. 7 and 8 with various DZ parameters, respectively. The effect of the plasma environment is to appreciably reduce cross sections just above threshhold.

Davis and Blaha (1982) have also investigated the same excitation processes for a impurity neon as those examined by Hatton et. al. (1981). They took an electrostatic potential of the charged particles Ze as

$$V(r) = Zer^{-1} - 4\pi e\,[r^{-1}\int_0^r r'^2 (\rho_b + \rho_f + \rho_i)\,dr' + \int_r^\infty r'(\rho_b + \rho_f + \rho_p)\,dr'] . \tag{41}$$

The positive charge distribution ρ_i was assumed to be

$$\rho_i = \rho_\infty \exp(-eV(r)/kT) \tag{42}$$

where V(r) is given in Eq. (40) and ρ_∞ is the average charge density in plasma. The free electron density with wavevector $\vec{k}$ is considered to be distributed in the Fermi statistical law of Eq. (11). By solving the two sets of the Schrödinger equations for the bound and the free electrons self-consistently, the scattering lengths for excitation processes of the $1s \rightarrow 2s$ and the $1s \rightarrow 2p$ were obtained. The calculated collision strength at T_e=200 eV is also reduced near the threshhold.

3-f) Stopping Power

In recent years there has been a growing interest in the stopping power in hot, dense plasma, since ion beams are also be used as an ICF driver. Recently the stopping power for some heavy ions in various cold target materials has been measured by Bimbot et. al. (1980) with the ion energies up to 5 MeV/amu and by Hubert et. al. (1980) with those 2.5-100 MeV/amu. Some of these results are quite different from those of Northcliffe et. al. (1970).

The dominant mechanism of the stopping power in a plasma is the energy loss of the projectile ion through the collision with plasma electrons in the Debye sphere and the excitation of plasmons out of the sphere. Mehlhorn (1981) and Meyer-ter-Vehn and Metzher (1981) have extended the standard theory of the stopping power for cold materials by Jackson (1962) to the partially ionized dense plasmas. The total stopping power S for a plasma can be expressed as a sum of the bound-electron S_b , free-electron S_f and plasma-ion S_i stopping powers:

$$S = S_b + S_f + S_i \quad . \tag{43}$$

The stopping power of the bound electrons S_b is written as

$$S_b = \text{Min.}\ (S_{Bethe}, S_{LSS}) + S_{nucl} \ , \qquad (44)$$

where S_{nucl} denotes the nuclear stopping power. The notation of Min. (S_{Bethe} , S_{LSS}) in Eq. (44) indicates the smaller value between the stopping-power formula of Bethe S_{Bethe} and the formula of Lindhard, Scharff and Schiott (1963) S_{LSS}. S_{Bethe} accounts for both ionizations and excitaions of the atomic electrons, whereas S_{LSS} , which is derived by use of the imaginary part of the dielectric function for the electron gas, calculates the electronic stopping power for low-energy projectile ions. When a heavy projectile ion with the very low incident energy passes through the plasma of heavy elements, the slowdown of the incident ion due to the elastic Coulomb collisions with the plasma ions becomes significant. In this case, the nuclear stopping power S_{nucl} is not neglected as a small value compared with the electronic stopping power. The differece of the theory between Mehlhorn and Meyer-ter-Vehn et. al. lies in the use of different effective charge q_{eff} of the projectile ion appearing in S_{Bethe}: The stopping power increases in proportion to the square of q_{eff}. Using Jackson' formula, Mehlhorn (1981) has also given the formulae for the stopping power of free plasma electrons S_f and of the plasma ions S_i in the binary collision theory.

Recently Maynard et. al. (1982) have proposed a method to calculate the electronic stopping power for nonrelativistic charged particles in dense electron fluids by using the exact random-phase-approximation (RPA) dielectric function. This approach implicitly contains both binary and collective processes. Maynard et. al. have given some numerical examples for the stopping power of very dense electron fluids, which is shown in Fig. 9. This figure shows that the temperature effect is important for ions with a few MeV per nucleon around $T_e \simeq \varepsilon_F$. As is expected, the stopping power is a decreasing function of the temperature.

The theoretical stopping powers obtained as a scaled form with respect to the atomic number of the projectile ion and/or the plasma ions described above are not compared with experiment yet.

Aknowledgement

The authors thank the members of the working group for atomic processes in hot, dense plasma, Profs. T. Fujimoto, Y. Itikawa, T. Nakamura, H. Tawara and K. Yonei and Drs. J. Hama, N. Miyanaga, N. Yamaguchi and K. Yamamoto for valuable comments.

References

Biomot R, Gardes D, Geissel H, Kitahara T, Aermbruster P, Fleury A and Hubert F (1980): Nucl. Inst. Meth. 174, 231.

Cauble R (1982): J. Quant. Spectrosc. Radiat. Trans. 28, 41.

Chandraseker S (1939): An Introduction to the Study of Stellar Structure (Dover).

Cowan R D and Ashkin J (1957): Phys. Rev. 105, 144.

Davis J and Blaha M (1982): J. Quant. Spectrosc. Radiat. Trans. 27, 307.

Feynman R P, Metropolis N and Teller E (1949): Phys. Rev. 75, 1561.

Grant I P (1958): Mon. Not. Roy. Astron. Soc. 118, 241.

Griem H R (1974): Spectral Line Broadening by Plasmas (Academic).

Gupta U and Rajagopal A K (1979): J. Phys. B12, L703.

________________ (1981): J. Phys. B14, 2309.

________________ (1982): Phys. Rept. 87, 259.

Hatton G J, Lane N F and Weisheit J C (1981): J. Phys. B14, 4879.

Höhne F E and Zimmermann R (1982): J. Phys. B15, 2551.

Hubert F, Fleury A, Bimbot R and Gardes D (1980): Ann. Phys. (Fr.) 5, 1.

Ichimaru S (1977): Strongly Coupled Plasmas, Eds. G. Kalman and P. Carini (Plenum) p. 187.

Jackson D (1962): Classical Electrodynamics (John Wiley & Sons).

Lamoureux M, Feng I J, Pratt R H and Tseng H K (1982): J. Quant. Spectrosc. Radiat. Trans. 27, 227.

Lindhard J, Scharff M and Schiott H E (1963): Kgl. Danske Videnskab. Selskab. Mat. Fys. Medd. 33, No. 14.

Maynard G and Deutsch C (1982): Phys. Rev. A26, 665.

Mehlhorn T A (1981): J. Appl. Phys. 52, 6522.

Meyer-ter-Vehn J and Metzler N (1981): Target Design for Heavy Ion Beam Fusion, Max-Planck-Institut für Quantenoptik, MPQ 48.

More R M (1981): Lawrence Livermore National Laboratory Report.

Nakayama T and DeWitt H (1964): J. Quant. Spectrosc. Radiat. Trans. 4, 623.

Northcliffe L C and Schilling R F (1970): Nucl. Data Tables A7, 233.

Rogers F J, Graboske Jr. H C and Harwood D J (1970): Phys. Rev. A1, 1577.

Roussel K M and O'Connell R F (1974): Phys. Rev. A9, 52.

Rozsnyai B F (1972): Phys. Rev. A5, 1137.

____________ (1975): J. Quant. Spectrosc. Radiat. Trans. 15, 695.

____________ (1979): J. Quant. Spectrosc. Radiat. Trans. 22, 337.

Shore B W (1975): J. Phys. B8, 2023.

Singwi K S (1977): Strongly Coupled Plasmas, Eds. G. Kalman and P. Carini (Plenum) p. 259.

Skupsky S (1980): Phys. Rev. A21, 1316.

Stwert J C and Pyatt K D (1966): Astrophys. J. 144, 1203.

Weisheit J C (1981): Princeton Plasma Physics Laboratory Report 1765.

Weisheit J C and Shore B W (1974): Astrophys. J. 194, 519.

Wigner E P (1948): Phys. Rev. 73, 1002.

Yamamoto K and Narumi H (1980): Prog. Theor. Phys. 64, 436.

Figure Captions

<u>Fig. 1</u> Dependence of the energy levels on the screening lengths for the six lowest-lying states (Rogers et. al. 1970).

<u>Fig. 2</u> Dependence of the energy levels on the screening lengths for some of the higher-lying states (Rogers et. al. 1970).

<u>Fig. 3</u> Spontaneous-emission transition probabilities in the dipole approximation for the Debye-Hückel (DH) potential is shown as a function of the DH screening length (Roussel et. al. 1974).

<u>Fig. 4</u> Averaged oscillator strengths $\sigma_{n\ell}(\omega)$ for the Debye-Hückel potential for different values of D and R, respectively (Höhne et. al. 1982): Crosses, σ at discrete lines; full curve, continuum. The monotonically decreasing curves show the Coulomb function $\sigma_{n\ell}^{Coul}(\omega)$. Arrows denote the line positions of the unscreened Coulomb potential. Note the shifted zero for different parameters.

<u>Fig. 5</u> Lyman-α line shift for neon impurity in a dense plasma at kT=750 eV (Gupta et. al. 1982). S-Skupsky (1980); DH-'linearized Debye-Huckel' (Skupsky 1980); NLDH-'non-linear Debye-Hückel' (Gupta et. al. 1981); open circles-V_{eff} (Gupta et. al. 1981); solid curve-Cauble (1982).

Fig. 6 Gaunt factors for cesium at 1 keV temperature and 1.9 g/cm^3 density, as a function of the fraction $h\nu/W_0$ of incident energy radiated by the photon (W_0=1 keV) (Lamoureux et. al. 1982). Dotted line (...): Coulomb Born approximation result G^B; dashed line (----): Born approximation result G^B_{SCFAA} from the SCFAA potential V_{SCFAA} of Rozsnyai (1979); solid line (——) : relativistic partial wave expansion results using the Thomas-Fermi potential V_{TF}; dash-dotted line (-·-): realtivistic partial wave expansion results using V_{SCFAA}.

Fig. 7 Total collision strengths $Z^2\Omega$ as a function of energy E/Z^2 (in a.u.) for the 1s→2s transition for screening lengths DZ=10, 20, 50, 100 and ∞ a_0 (——) (Hatton et. al. 1981). Results corresponding to screened target-state energies for DZ=10 a_0 and 20 a_0 (-----) are above the respective unscreened energies curves. CBI results for Z=2 are also shown.

Fig. 8 Total collision strengths $Z^2\Omega$ as a function of energy E/Z^2 (in a.u.) for the 1s→2p transition for screening lengths DZ=10, 20, 50, and ∞ a_0 (——) (Hatton et. al. 1981). Results corresponding to screened target-state energies for DZ=10 a_0 (closed circles) are above the respective unscreened energies curves. CBI results for Z=2 are also shown.

Fig. 9 Stopping power dE/dx (a.u.) at $N_e=10^{25}$/cm^3 and various temperatures (Maynard et.al. 1982).

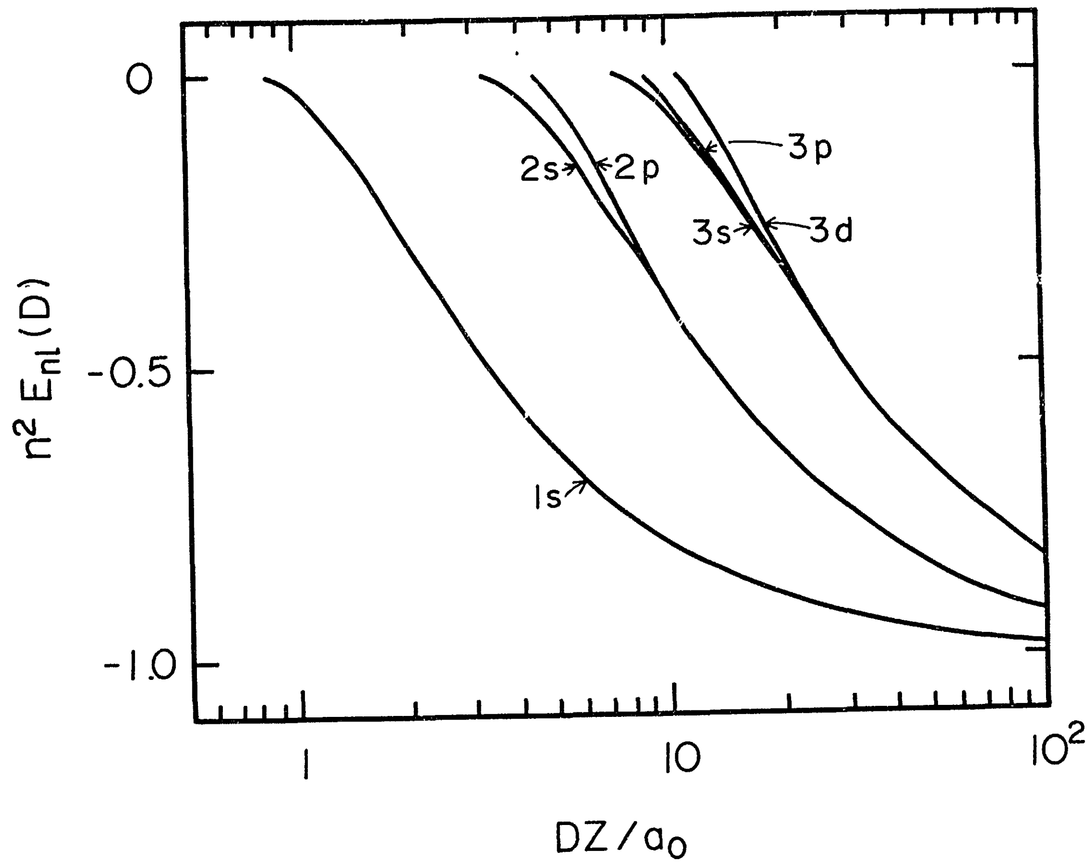

0
-0.5
-1.0
$n^2 E_{nl}(D)$
1s
2s
2p
3s
3p
3d
1
10
10^2
DZ/a_0

Fig. 1

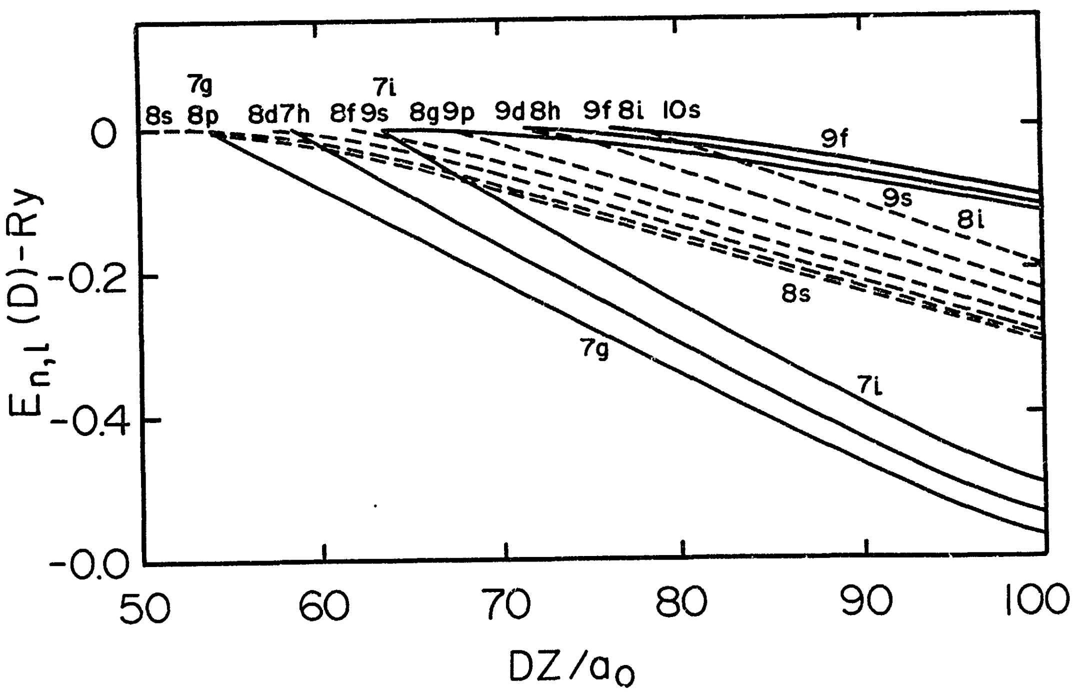

8s
7g
8p
8d
7h
8f
7i
9s
8g
9p
9d
8h
9f
8i
10s
9f
9s
8i
8s
7g
7i
0
-0.2
-0.4
-0.0
$E_{n,l}(D)$-Ry
50
60
70
80
90
100
DZ/a_0

Fig. 2

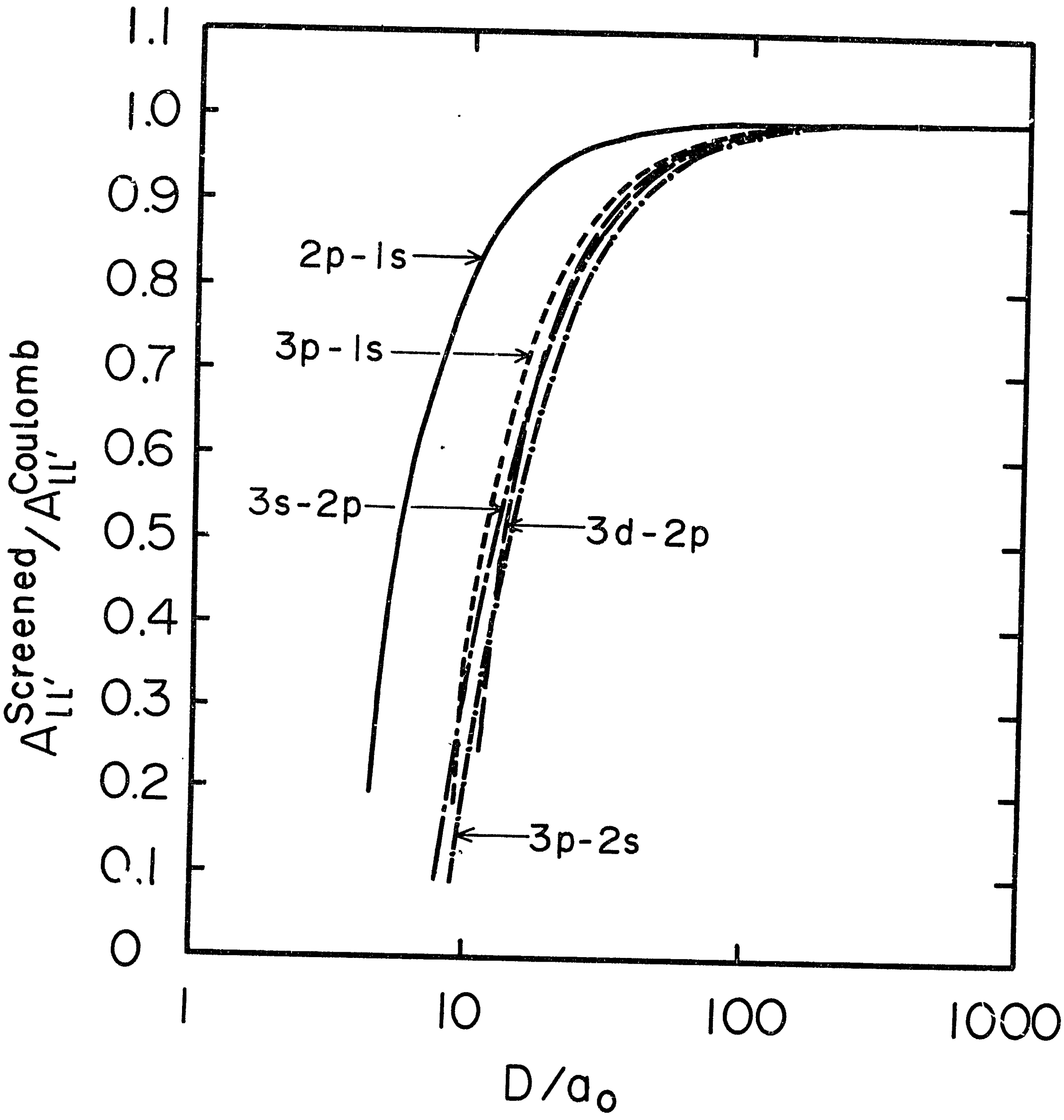

1.1
1.0
0.9
0.8
0.7
0.6
0.5
0.4
0.3
0.2
0.1
0
1
10
100
1000
$A_{ll'}^{Screened}/A_{ll'}^{Coulomb}$
D/a_0
2p-1s
3p-1s
3s-2p
3d-2p
3p-2s

Fig. 3

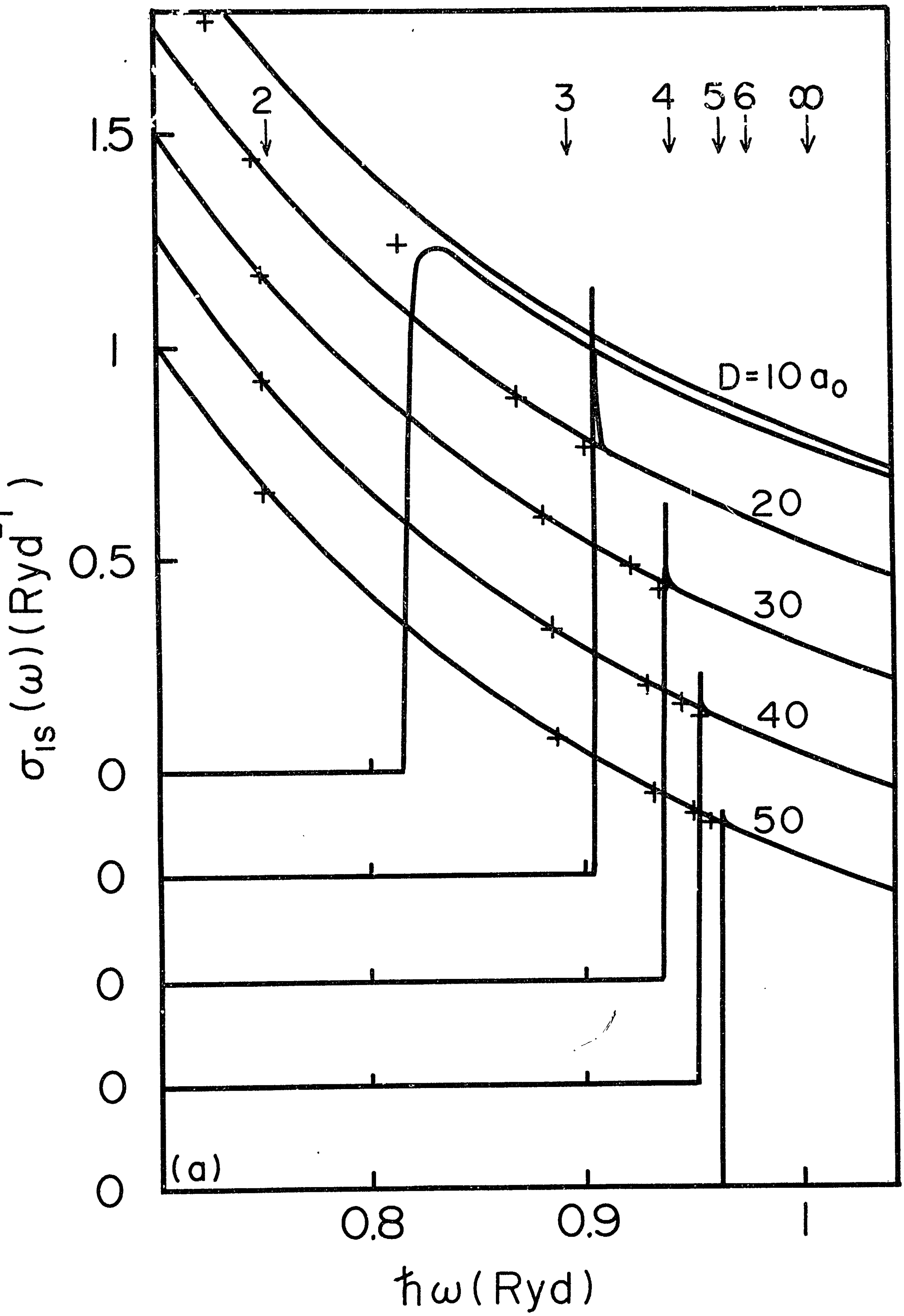

Fig. 4

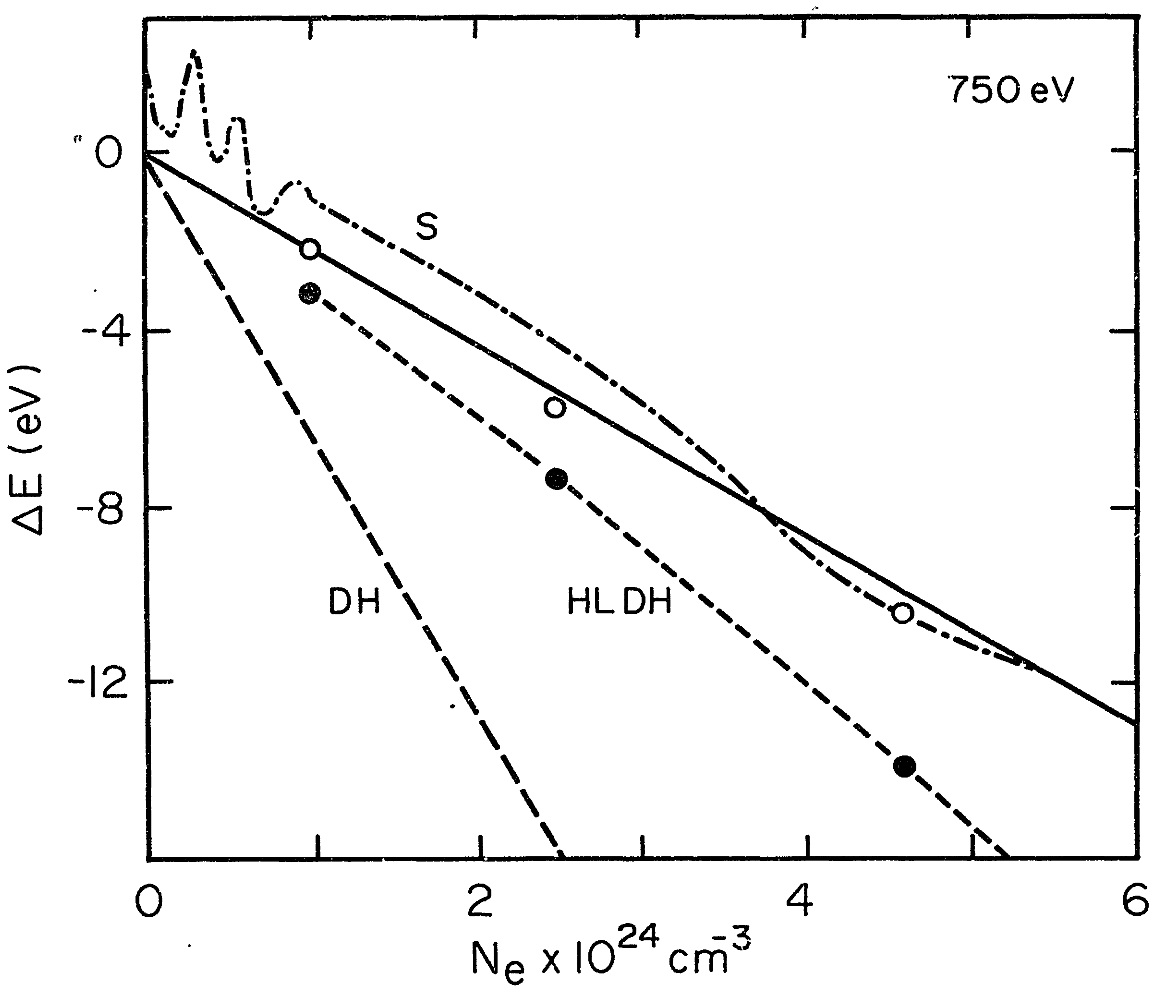

Fig. 5

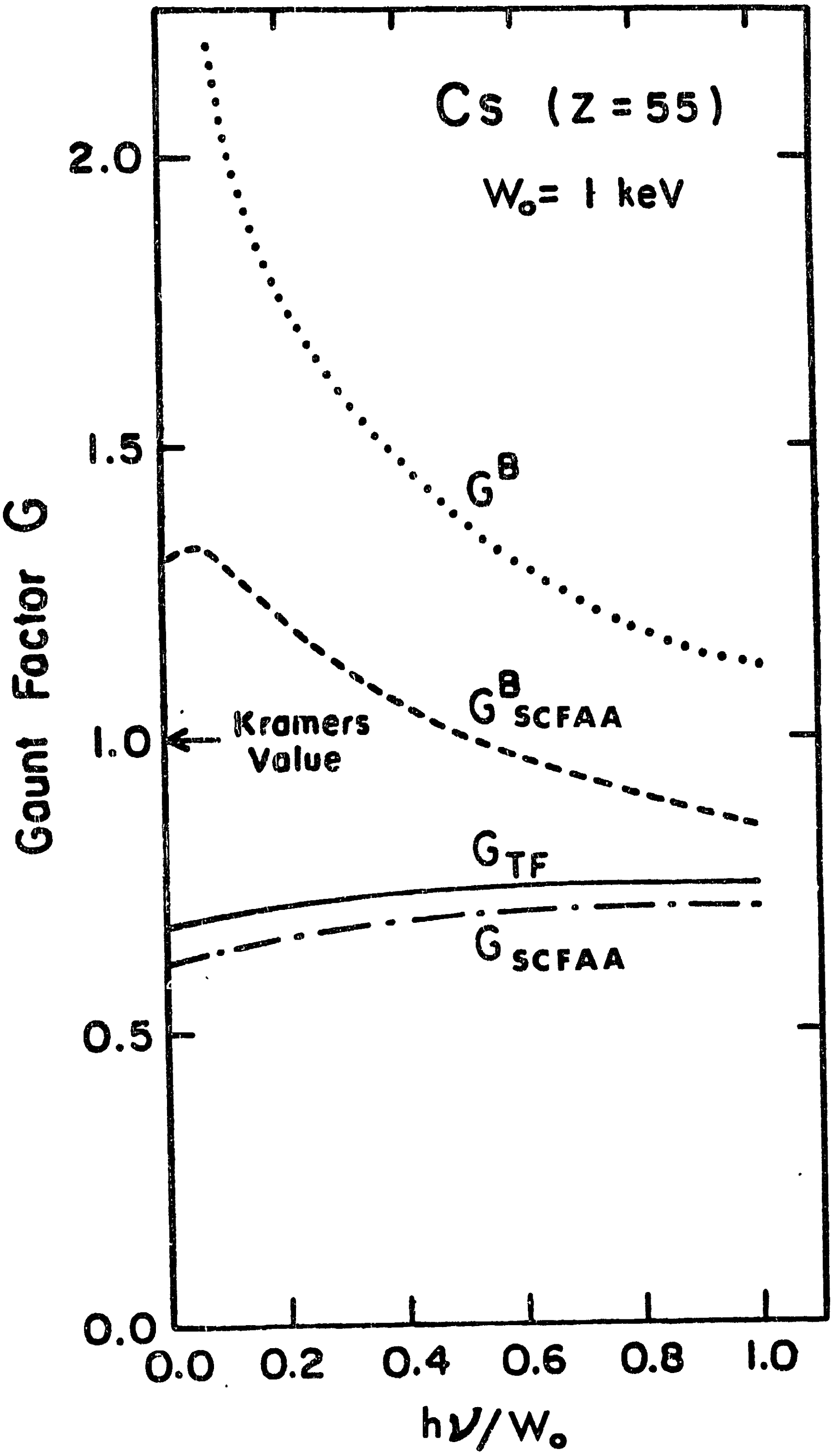

Cs (Z = 55)
W_o= 1 keV
G^B
G^B_{SCFAA}
Kramers Value
G_{TF}
G_{SCFAA}
Gaunt Factor G
2.0
1.5
1.0
0.5
0.0
0.0
0.2
0.4
0.6
0.8
1.0
$h\nu/W_o$

Fig. 6

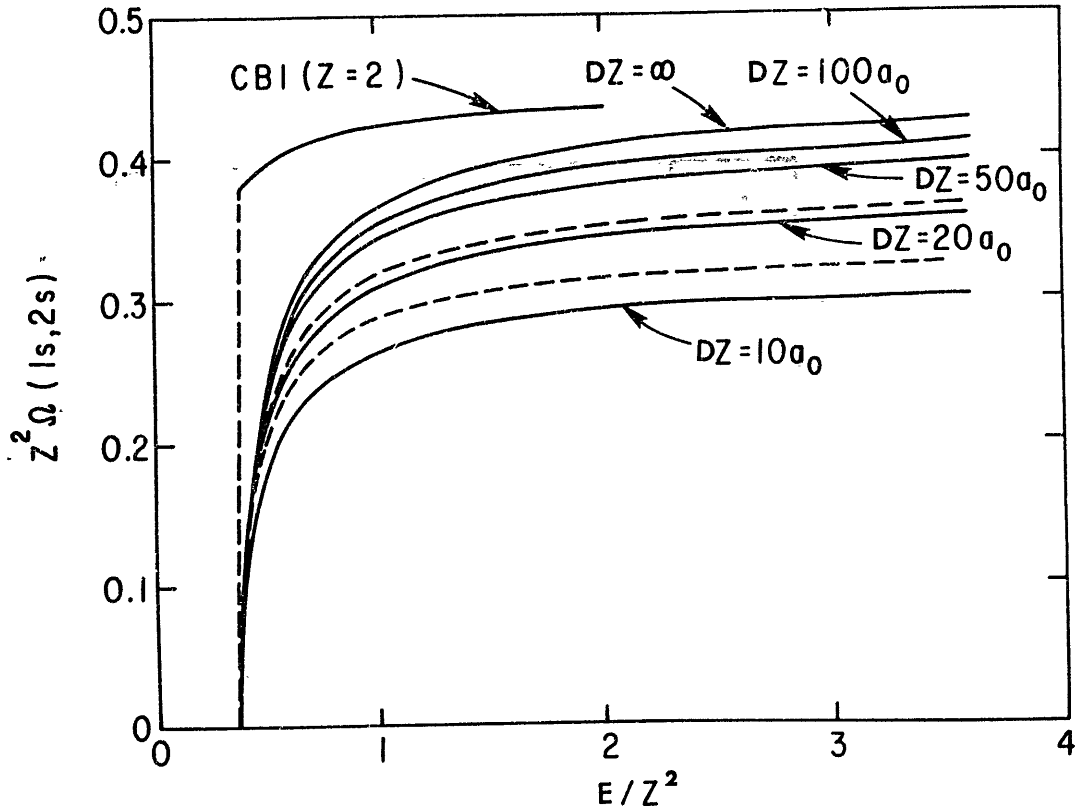
0.5
0.4
0.3
0.2
0.1
0
$Z^2\Omega$ (1s,2s)
0
1
2
3
4
E/Z^2
CBI (Z = 2)
DZ = ∞
DZ = $100a_0$
DZ = $50a_0$
DZ = $20a_0$
DZ = $10a_0$

Fig. 7

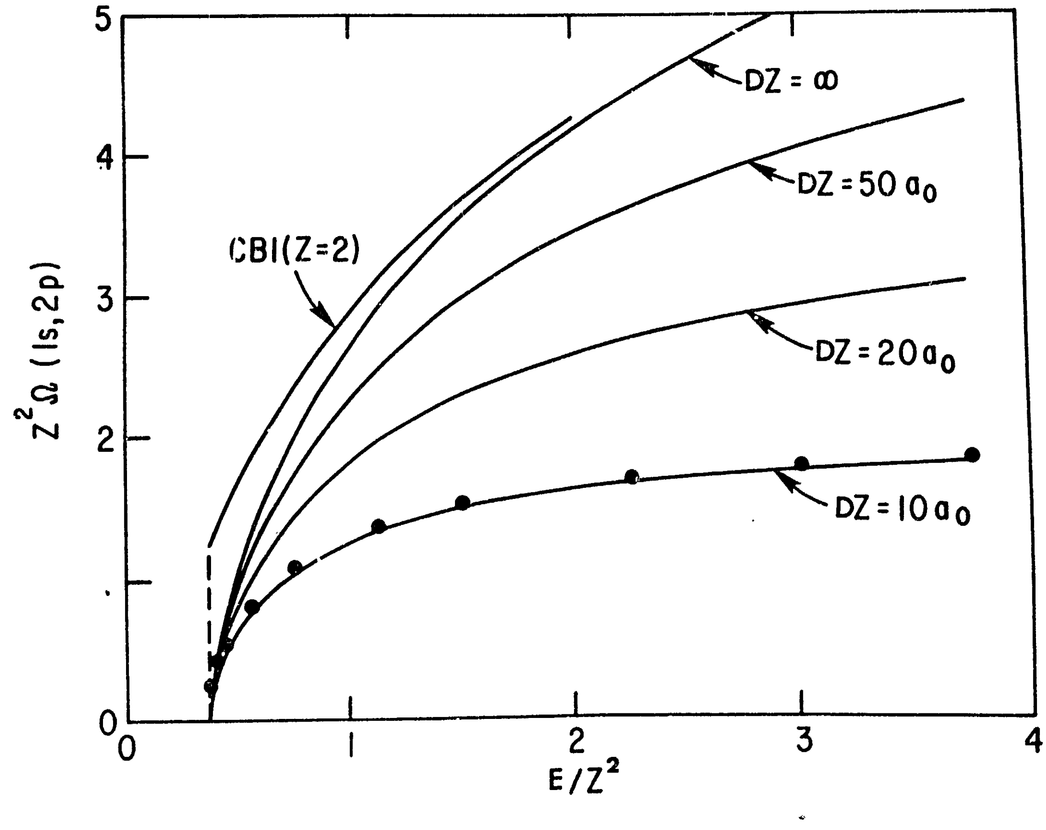
5
4
3
2
0
$Z^2\Omega$ (1s,2p)
0
1
2
3
4
E/Z^2
DZ = ∞
DZ = 50 a_0
CBI(Z=2)
DZ = 20 a_0
DZ = 10 a_0

Fig. 8

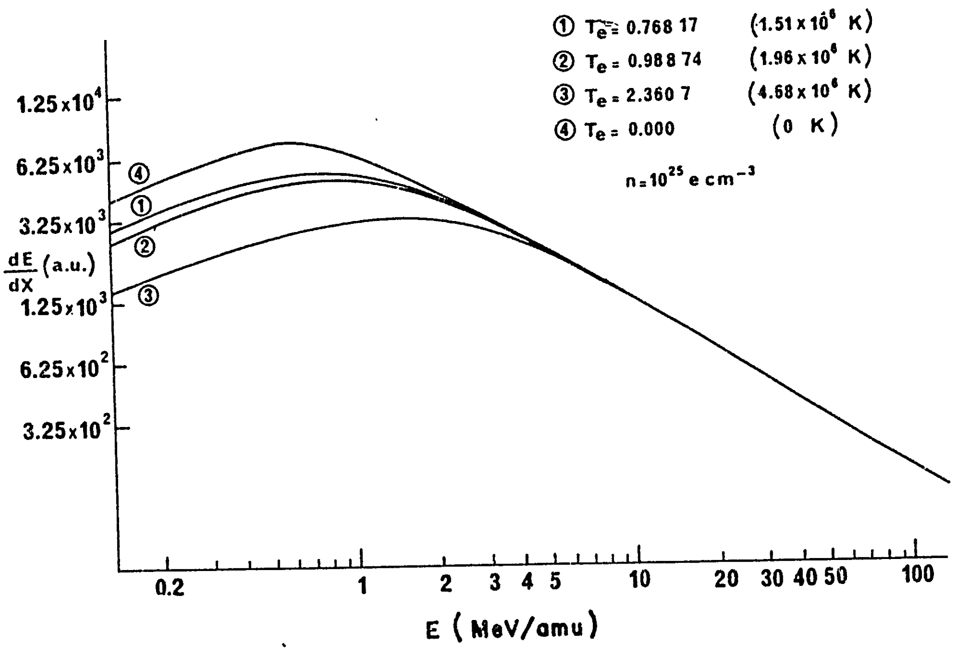
① T_e = 0.768 17 (1.51 x 10^6 K)
② T_e = 0.988 74 (1.96 x 10^6 K)
③ T_e = 2.360 7 (4.68 x 10^6 K)
④ T_e = 0.000 (0 K)
$n = 10^{25}$ e cm^{-3}
1.25 x 10^4
6.25 x 10^3
3.25 x 10^3
$\frac{dE}{dX}$ (a.u.)
1.25 x 10^3
6.25 x 10^2
3.25 x 10^2
0.2
1
2
3
4
5
10
20
30
40
50
100
E (MeV/amu)

Fig. 9

LIST OF IPPJ-AM REPORTS

IPPJ-AM-1* "Cross Sections for Charge Transfer of Hydrogen Beams in Gases and Vapors in the Energy Range 10 eV–10 keV"
H. Tawara (1977) [Published in Atomic Data and Nuclear Data Tables 22, 491 (1978)]

IPPJ-AM-2* "Ionization and Excitation of Ions by Electron Impact –Review of Empirical Formulae–"
T. Kato (1977)

IPPJ-AM-3 "Grotrian Diagrams of Highly Ionized Iron FeVIII-FeXXVI"
K. Mori, M. Otsuka and T. Kato (1977) [Published in Atomic Data and Nuclear Data Tables 23, 196 (1979)]

IPPJ-AM-4 "Atomic Processes in Hot Plasmas and X-Ray Emission"
T. Kato (1978)

IPPJ-AM-5* "Charge Transfer between a Proton and a Heavy Metal Atom"
S.Hiraide, Y. Kigoshi and M. Matsuzawa (1978)

IPPJ-AM-6* "Free-Free Transition in a Plasma –Review of Cross Sections and Spectra–"
T. Kato and H. Narumi (1978)

IPPJ-AM-7* "Bibliography on Electron Collisions with Atomic Positive Ions: 1940 Through 1977"
K. Takayanagi and T. Iwai (1978)

IPPJ-AM-8 "Semi-Empirical Cross Sections and Rate Coefficients for Excitation and Ionization by Electron Collision and Photoionization of Helium"
T. Fujimoto (1978)

IPPJ-AM-9 "Charge Changing Cross Sections for Heavy-Particle Collisions in the Energy Range from 0.1 eV to 10 MeV I. Incidence of He, Li, Be, B and Their Ions"
Kazuhiko Okuno (1978)

IPPJ-AM-10 "Charge Changing Cross Sections for Heavy-Particle Collisions in the Energy Range from 0.1 eV to 10 MeV II. Incidence of C, N, O and Their Ions"
Kazuhiko Okuno (1978)

IPPJ-AM-11 "Charge Changing Cross Sections for Heavy-Particle Collisions in the Energy Range from 0.1 eV to 10 Mev III. Incidence of F, Ne, Na and Their Ions"
Kazuhiko Okuno (1978)

IPPJ-AM-12* "Electron Impact Excitation of Positive Ions Calculated in the Coulomb-Born Approximation –A Data List and Comparative Survey–"
S. Nakazaki and T. Hashino (1979)

IPPJ-AM-13 "Atomic Processes in Fusion Plasmas – Proceedings of the Nagoya Seminar on Atomic Processes in Fusion Plasmas Sept. 5-7, 1979"
Ed. by Y. Itikawa and T. Kato (1979)

IPPJ-AM-14 "Energy Dependence of Sputtering Yields of Monatomic Solids"
N. Matsunami, Y. Yamamura, Y. Itikawa, N. Itoh, Y. Kazumata, S. Miyagawa, K. Morita and R. Shimizu (1980)

IPPJ-AM-15 "Cross Sections for Charge Transfer Collisions Involving Hydrogen Atoms"
Y. Kaneko, T. Arikawa, Y. Itikawa, T. Iwai, T. Kato, M. Matsuzawa, Y. Nakai, K. Okuno, H. Ryufuku, H. Tawara and T. Watanabe (1980)

IPPJ-AM-16 "Two-Centre Coulomb Phaseshifts and Radial Functions"
H. Nakamura and H. Takagi (1980)

IPPJ-AM-17 "Empirical Formulas for Ionization Cross Section of Atomic Ions for Electron Collisions —Critical Review with Compilation of Experimental Data—"
Y. Itikawa and T. Kato (1981)

IPPJ-AM-18 "Data on the Backscattering Coefficients of Light Ions from Solids"
T. Tabata, R. Ito, Y. Itikawa, N. Itoh and K. Morita (1981)

IPPJ-AM-19 "Recommended Values of Transport Cross Sections for Elastic Collision and Total Collision Cross Section for Electrons in Atomic and Molecular Gases"
M. Hayashi (1981)

IPPJ-AM-20 "Electron Capture and Loss Cross Sections for Collisions between Heavy Ions and Hydrogen Molecules"
Y. Kaneko, Y. Itikawa, T. Iwai, T. Kato, Y. Nakai, K. Okuno and H. Tawara (1981)

IPPJ-AM-21 "Surface Data for Fusion Devices – Proceedings of the U.S–Japan Workshop on Surface Data Review Dec. 14-18, 1981"
Ed. by N. Itoh and E.W. Thomas (1982)

IPPJ-AM-22 "Desorption and Related Phenomena Relevant to Fusion Devices"
Ed. by A. Koma (1982)

IPPJ-AM-23 "Dielectronic Recombination of Hydrogenic Ions"
T. Fujimoto, T. Kato and Y. Nakamura (1982)

IPPJ-AM-24 "Bibliography on Electron Collisions with Atomic Positive Ions: 1978 Through 1982 (Supplement to IPPJ-AM-7)"
Y. Itikawa (1982)

IPPJ-AM-25 "Bibliography on Ionization and Charge Transfer Processes in Ion-Ion Collision"
H. Tawara (1983)

IPPJ-AM-26 "Angular Dependence of Sputtering Yields of Monatomic Solids"
Y. Yamamura, Y. Itikawa and N. Itoh (1983)

IPPJ-AM-27 "Recommended Data on Excitation of Carbon and Oxygen Ions by Electron Collisions"
Y. Itikawa, S. Hara, T. Kato, S. Nakazaki, M.S. Pindzola and D.H. Crandall (1983)

IPPJ-AM-28 "Electron Capture and Loss Cross Sections for Collisions Between Heavy Ions and Hydrogen Molecules (Up-dated version of IPPJ-AM-20)
H. Tawara, T. Kato and Y. Nakai (1983)

IPPJ-AM-29 "Bibliography on Atomic Processes in Hot Dense Plasmas"
T. Kato, J. Hama, T. Kagawa, S. Karashima, N. Miyanaga, H. Tawara, N. Yamaguchi, K. Yamamoto and K. Yonei (1983)

IPPJ-AM-30 "Cross Sections for Charge Transfers of Highly Ionized Ions in Hydrogen Atoms (Up-dated version of IPPJ-AM-15)"
H. Tawara, T. Kato and Y. Nakai (1983)

IPPJ-AM-31 "Atomic Processes in Hot Dense Plasmas"
T. Kagawa, T. Kato, T. Watanabe and S. Karashima (1983)

Available upon request to Research Information Center, Institute of Plasma Physics, Nagoya University, Nagoya 464, Japan, except for the reports noted with*.